Available online at www.sciencedirect.com
ScienceDirect
Journal of Power Sources 162 (2006) 644–650
JOURNAL OF POWER SOURCES
www.elsevier.com/locate/jpowsour

Investigation and improvement on the storage property of $LiNi_{0.8}Co_{0.2}O_2$ as a cathode material for lithium-ion batteries

Hansan Liu [a,b], Yong Yang [a,*], Jiujun Zhang [b,**]

[a] State Key Laboratory for Physical Chemistry of Solid Surfaces, Department of Chemistry, Xiamen University, Xiamen 361005, PR China
[b] Institute for Fuel Cell Innovation, National Research Council of Canada, Vancouver, BC V6T 1W5, Canada

Received 8 July 2006; received in revised form 17 July 2006; accepted 18 July 2006
Available online 22 August 2006

Abstract

$LiNi_{0.8}Co_{0.2}O_2$ cathode material showed a performance loss after storage in air. The surface species on the material formed during the exposure to air were identified through TG, SEM, TPD-MS, XRD and XPS. Two thin layers were found on the surface. The first layer in contact with the bulk material contains NiO-like species, and the top layer consists of adsorbed hydroxyl, bicarbonate, carbonate, and crystalline Li_2CO_3. These two layers are both electrochemically inactive and poor conductors for Li^+ ions, which are believed to be responsible for the storage loss. A chemical reaction mechanism, involving atmospheric H_2O and CO_2, and the particle surface of $LiNi_{0.8}Co_{0.2}O_2$ material, was proposed to explain the formation process of those surface species. For storage loss prevention, a doping approach to reduce nickel content and a storage approach to isolate the material from H_2O and CO_2 were found to be effective to improve the storage property of $LiNiO_2$-based materials. For storage loss recovery, a heat-treatment process at 725 °C was demonstrated to be a feasible approach for full recovery of the performance.

Keywords: $LiNi_{0.8}Co_{0.2}O_2$; Storage property; Cathode material; Lithium-ion battery; Surface analysis

1. Introduction

In recent years, rechargeable lithium-ion batteries are successfully used in portable, entertainment, computing and telecommunication devices. However, a challenge for new generation lithium-ion batteries is to develop new cathode materials to replace the currently used material such as $LiCoO_2$, which is expensive, toxic and has low capacity [1]. Among several alternative materials, $LiNiO_2$-based compounds have shown promising in terms of lower cost and higher capacity. With respect to practical applications, many works have focused on structural modification and composition optimization to improve the performance of $LiNiO_2$ and its derivates [2–5]. The storage property of $LiNiO_2$-based materials, which is directly related to the material production, electrode fabrication and battery operation, has attracted considerable attention recently [6–12].

The formation of Li_2CO_3 on the surface was thought to be the main source of poor storage property of $LiNiO_2$-based materials [8–11]. It has been found that lithium carbonate is not only electrochemically inactive due to poor electronic conductivity and low Li^+ conductivity, but also easily causes gas evolution during the battery operation [8]. Zhuang et al. [9] found that a 10 nm thin layer of Li_2CO_3 was formed on $LiNi_{0.8}Co_{0.15}Al_{0.05}O_2$ particles after 2-year storage and resulted in a much lower capacity than that of fresh ones. Kim et al. [10] observed a serious cell swelling of a Li-ion battery at a charged state of 4.2 V, and attributed that to the existence of Li_2CO_3 and LiOH on the $LiNi_{0.8}Co_{0.15}Al_{0.05}O_2$ cathode material surface. The formation of Li_2CO_3 during storage is usually attributed to the presence of H_2O and CO_2 in air. Trace amounts of H_2O and CO_2 in air could adsorb on the material particle surface to react with lithium ions to form a layer of lithium carbonate. In addition, the formation of Li_2CO_3 on the material surface has been found to be strongly dependent on the chemical stability of the substrate material ($LiNiO_2$) during storage [12].

However, our recent results showed that Li_2CO_3 is not the only surface species on the stale material and also not the sole species causing the performance loss. Therefore, a deeper under-

* Corresponding author. Tel.: +86 592 2185753; fax: +86 592 2185753.
** Corresponding author. Tel.: +1 604 221 3087; fax: +1 604 221 3001.
E-mail addresses: yyang@xmu.edu.cn (Y. Yang), jiujun.zhang@nrc.gc.ca (J. Zhang).

0378-7753/$ – see front matter.
doi:10.1016/j.jpowsour.2006.07.028

standing of the surface changes during storage is necessary for clarifying the mechanism of such poor storage property of $LiNiO_2$-based materials. On the other hand, the prevention and recovery of the storage loss, which have not been emphasized in the literature, are other important aspects of research and development of the cathode materials.

In this paper, the surface changes on the cathode material of $LiNi_{0.8}Co_{0.2}O_2$ after long-term exposure to air were analyzed by thermal gravitometer (TG), scanning electron microscope (SEM), temperature programmed desorption-mass spectroscopy (TPD-MS), X-ray photoelectron spectroscopy (XPS) and X-ray diffraction (XRD). Several coin-type lithium-ion batteries assembled using the cathode materials before and after storage and post-treatment were tested and diagnosed for electrochemical performance characterization. Some approaches to improve the storage property and recover the degraded performance of $LiNi_{0.8}Co_{0.2}O_2$ cathode material were explored as well.

2. Experimental section

2.1. Material preparation

The cathode materials ($LiNiO_2$, $LiNi_{0.8}Co_{0.2}O_2$, $LiNi_{0.75}Co_{0.2}Ti_{0.05}O_2$ and $LiCoO_2$) were synthesized by a sol–gel method using citric acid as a chelating agent, as reported in our previous work [13,14]. The storage process was carried out at room temperature by storing the sample in air, or in an argon-filled glove box (Master 100 Lab, M. Braun, Germany) for 6 months. For the heat-treatment, two stored $LiNi_{0.8}Co_{0.2}O_2$ samples were heated with a 500 sccm oxygen flow at 500 and 725 °C for 1 h, respectively.

2.2. Physical characterization

TG experiments were carried out on a Netzsch STA 400 analyzer (Germany) with 100 ml min^{-1} of flowing N_2 gas and a heating rate of 20 °C min^{-1} in the temperature range of 25–900 °C. SEM spectra were taken by a LEO 1530 Field Emission Scanning Electron Microscope (Oxford Instrument). A homemade temperature controlled system combined with a Qminstar QMS200 (USA) was employed for TPD-MS measurements, where helium gas (>99.999%) was used as a carrier. During TPD-MS measurements, the samples were heated in a range of 25–900 °C at a rate of 20 °C min^{-1} with a helium flow rate of 10 ml min^{-1}. Three desorbed species, H_2O ($m/e = 18$), CO_2 ($m/e = 44$) and O_2 ($m/e = 32$), were analyzed by mass spectroscopy. XPS analysis was performed using a Physical Electronics Quantum 2000 ESCA spectrometer (USA) with monochromatic Al Kα 1486.6 eV radiation operated at 23.2 W in a vacuum of $<10^{-8}$ Torr. The binding energy was calibrated with reference to the C 1s level of hydrocarbon (284.6 eV). XRD measurements were carried out on a Rigaku Rotaflex D/max-C diffractometer (Japan) with graphite monochromator and Cu Kα radiation operated at 40 kV and 30 mA. Data were collected in the range 10–90° using a step scan method with a step size of 0.02° and a counting time of 2 s per step. Rietveld refinement structural analysis was operated using general structure analysis system (GSAS) [15].

2.3. Electrochemical measurements

Electrochemical evaluation of the cathode samples was carried out using CR2025 lithium-ion coin cell hardware. The cathodes were made by a blade technique after mixing 85% of the active material with 10% carbon black and 5% PVDF using NMP as a solvent. The cell was assembled with a prepared cathode, an anode (lithium metal), a separator (Celgard 2300 film), and the electrolyte (1 M $LiPF_6$ in EC + DMC (1:1)). Charge–discharge experiments were performed galvanostatically with a current density of 18 mA g^{-1} in the range of 3.0–4.2 V using an Arbin BT-2043 battery test system.

3. Results and discussion

3.1. Electrochemical performance before and after the storage

Fig. 1 shows the charge–discharge curves of the fresh and stored $LiNi_{0.8}Co_{0.2}O_2$ materials. Freshly synthesized $LiNi_{0.8}Co_{0.2}O_2$ sample has a charge specific capacity of 202 mAh g^{-1} and a discharge specific capacity of 180 mAh g^{-1} in the voltage range of 3.0–4.2 V at a current density of 18 mA g^{-1}. However, the performance of the sample decreases dramatically after storage in air for 6 months. The charge and discharge specific capacities dropped from 202 to 167 mAh g^{-1} and from 180 to 142 mAh g^{-1}, respectively. In the mean time, the charge curve is ~200 mV higher than that of the fresh sample, and the discharge curve is ~200 mV lower than that of the fresh sample, indicating a larger electrochemical polarization for the stored material. For comparison, one of the $LiNi_{0.8}Co_{0.2}O_2$ samples was also stored in an Ar atmosphere for 6 months. This stale sample shows a charge specific capacity of 190 mAh g^{-1} and a discharge specific capacity of 168 mAh g^{-1}, which are only slightly lower than those of a fresh one. It is not clear about this slight capacity loss at this moment. More sensitive methods

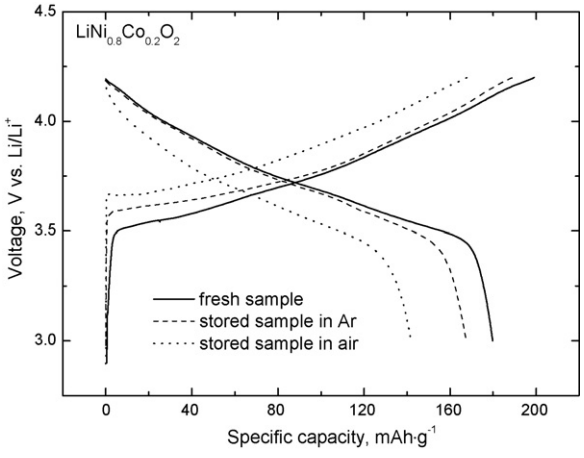

Fig. 1. Charge–discharge curves of $LiNi_{0.8}Co_{0.2}O_2$ cathode material: (solid line) fresh; (dash line) stored in Ar; (dot line) stored in air.

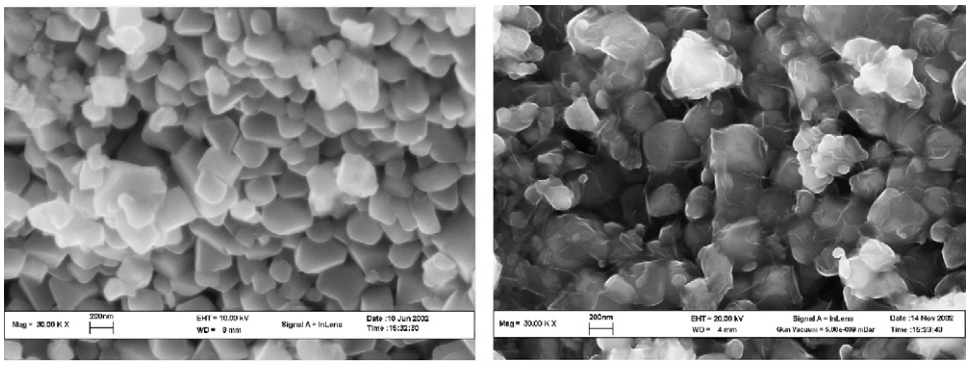

Fig. 2. SEM pictures of $LiNi_{0.8}Co_{0.2}O_2$ cathode material (a) before and (b) after storage in air.

may be necessary to detect the surface change of this cathode material during the storage in an Ar atmosphere. This result suggests that the performance degradation of the stored materials may be caused by the reactions between $LiNi_{0.8}Co_{0.2}O_2$ and the atmosphere. These reactions should include surface physical/chemical adsorption and possibly direct redox reactions between the bulk material and atmosphere components.

3.2. Determination of surface species

In order to clarify the origin of the performance loss, the surface species on the stored-in-air $LiNi_{0.8}Co_{0.2}O_2$ were identified by SEM, TG and TPD-MS techniques. Fig. 2 shows the SEM pictures of the fresh and stored $LiNi_{0.8}Co_{0.2}O_2$ materials. It can be seen that the fresh sample contains smooth particles with sharp edges in the range of 100–200 nm. For the stored sample, the particle morphology has obviously changed. The SEM picture shows a layer of transparent substance covering the particles. It was also observed that this transparent layer could change or partially disappear if the measurement time was long enough during the SEM operation. This phenomenon indicated that some weakly adsorbed surface species could come off the surface in an Ar environment.

To identify these surface species, TG measurements were carried out for the stored $LiNi_{0.8}Co_{0.2}O_2$ sample. Fig. 3 shows the results together with those taken from the stale materials of $LiCoO_2$ and $LiNiO_2$ for comparison. It is clear from Fig. 3 that $LiCoO_2$ has better thermal stability at high temperature than $LiNiO_2$. Generally, $LiNiO_2$ and $LiNi_{0.8}Co_{0.2}O_2$ begin to decompose after 800 °C, while $LiCoO_2$ remains stable over 900 °C [16]. The TG curve of the stale $LiCoO_2$ stayed almost constant up to 900 °C, suggesting that no surface species were formed on $LiCoO_2$ during storage in air. On the contrary, there are large weight losses in the TG curves of the stored $LiNiO_2$ and $LiNi_{0.8}Co_{0.2}O_2$ before the decomposition temperature of 800 °C. The weight losses of $LiNi_{0.8}Co_{0.2}O_2$ are relatively less than those of $LiNiO_2$, which could be due to the partial Ni substitution by Co. The poor storage property of $LiNiO_2$-based materials compared to $LiCoO_2$ may be attributed to the nature of the nickel element in the material.

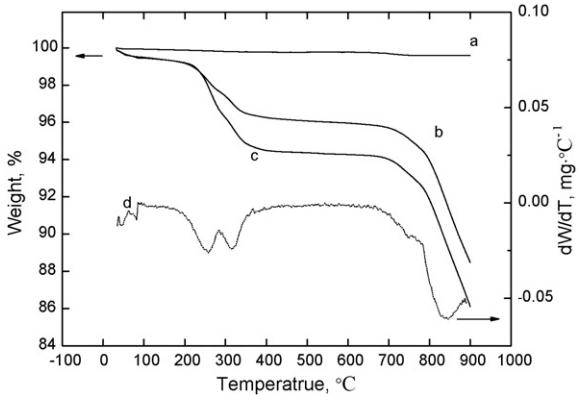

Fig. 3. TG curves of (a) $LiCoO_2$; (b) $LiNi_{0.8}Co_{0.2}O_2$; (c) $LiNiO_2$ after storage in air; (d) DTG curve of (b).

A DTG curve for $LiNi_{0.8}Co_{0.2}O_2$ is also shown in Fig. 3, from which four regions of weight loss can be identified. A small weight loss (~0.2%) occurs below 100 °C, which is due to the desorption of superficial water. Between 200 and 400 °C, there is a large weight loss of ~3.7%. Adsorbed species may contribute to the weight loss in this temperature range. Two desorption peaks can be observed in this region, indicating that two kinds of surface species are present on the stored material. Between temperatures 680 and 780 °C, another small weight loss of ~1.3% appears. Because the decomposition of Li_2CO_3 happens in this temperature range, this small downward wave could be attributed to the decomposition of Li_2CO_3. Up to 800 °C, a continuous drop of the curve can be observed, indicating the decomposition of $LiNiO_2$. These results suggest that Li_2CO_3 is not the main component on the surface of the stored $LiNi_{0.8}Co_{0.2}O_2$, and most surface species maybe ascribed to the adsorbed species.

To further identify the surface species on the stored $LiNi_{0.8}Co_{0.2}O_2$, TPD-MS experiments were carried out. Fig. 4 shows H_2O, CO_2 and O_2 TPD-MS spectra of the fresh and stored $LiNi_{0.8}Co_{0.2}O_2$. For CO_2-TPD-MS spectra, fresh $LiNi_{0.8}Co_{0.2}O_2$ does not show any desorbed peaks before decomposition. However, the spectrum of the stored sample shows three desorbed peaks before 800 °C. These adsorbed species may be attributed to various carbonate groups, which have different formation mechanisms. As reported in previous studies [17–19], chemisorptions of CO_2 on basic oxides can form various adsorbed carbonate, adsorbed bicarbonate and

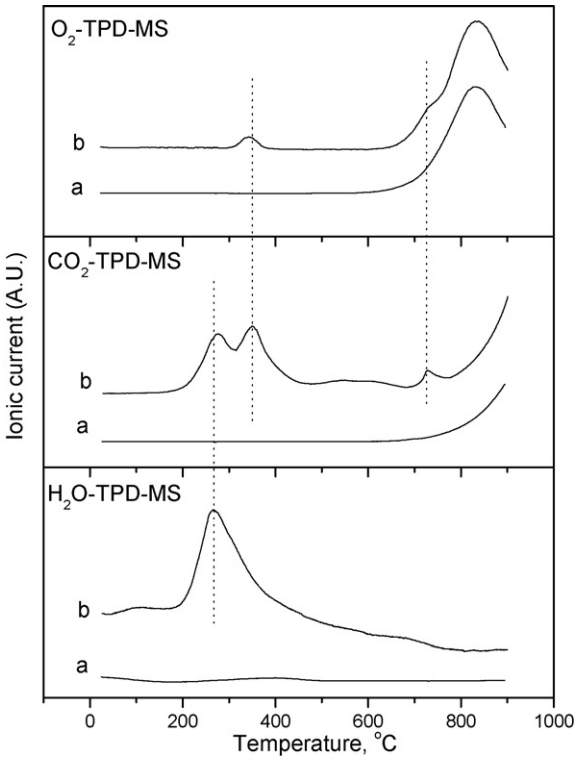

Fig. 4. H_2O-, CO_2- and O_2-TPD-MS spectra of $LiNi_{0.8}Co_{0.2}O_2$ material: (a) fresh; (b) stored in air.

ionic carbonate species. According to the thermal stability of these species [17–19], the peaks around 270, 350, and 725 °C can be attributed to adsorbed bicarbonate species, adsorbed carbonate species, and ionic carbonate species, respectively. These peaks are consistent with those peaks of the DTG curve in Fig. 3. In addition, it can be seen that the peak areas of adsorbed bicarbonate and carbonate species are much larger than that of ionic carbonate species, which is consistent with the result of weight losses shown on DTG curve. For H_2O-TPD-MS spectra, the fresh $LiNi_{0.8}Co_{0.2}O_2$ does not show an obvious desorbed peak, while the stored $LiNi_{0.8}Co_{0.2}O_2$ shows a broad desorbed peak around 270 °C. Since the temperature of this peak is at the temperature position of the first peak in CO_2-TPD-MS spectrum, the desorbed species at this temperature range may originate from the decomposition of adsorbed bicarbonate species. Meanwhile, chemisorbed hydroxyl may also contribute to this desorbed peak, because the H_2O-peak area is much larger than the peak area of the adsorbed bicarbonate species at the same temperature. For O_2-TPD-MS spectra, the stored sample shows two peaks before the decomposition temperature. Comparing O_2- to CO_2-TPD-MS spectra, it can be found that the temperatures of two O_2-desorbed peaks correspond well to those of two CO_2-desorbed peaks, indicating that O_2 at 350 and 725 °C may be the product of the decompositions of adsorbed carbonate and ionic carbonate species, respectively. Obviously, oxygen chemisorption from air should be excluded in this case, because these peaks do not appear in the fresh sample that has been sintered and cooled down under O_2 flow for a long time. Therefore, the oxygen source of these surface species probably originated from the bulk $LiNi_{0.8}Co_{0.2}O_2$. According to the surface chemistry of nickel oxides [20], some active oxygen species (O^-, O_2^-, etc.) are likely formed on the oxide surface. In TPD experiments [20], these active oxygen species can also be observed at the above-mentioned temperatures. Hence, it is reasonable to suggest that active oxygen species could be formed on the particle surface of $LiNi_{0.8}Co_{0.2}O_2$ during storage. These active oxygen species are susceptible to combine with CO_2 to form absorbed carbonate, and also combine with H_2O to form hydroxyl species that easily react with adsorbed CO_2 to produce absorbed bicarbonate species. Absorbed carbonate species could be evolved to ionic carbonate species in a Li^+-rich environment.

3.3. Determination of composition/structure changes

In order to demonstrate the formation of surface species identified above, the surface composition changes of the $LiNi_{0.8}Co_{0.2}O_2$ during storage in air were detected by XPS, as shown in Fig. 5. In the O 1s spectra, two peaks are observed for the fresh sample. The dominating one is located at 528.8 eV, which can be assigned to the lattice oxygen. Another small peak is located at the higher binding energy of 531.0 eV. This peak can be assigned to the active oxygen species on nickel oxides [21] or the impurity of adsorbed species. For the stored sample, the O 1s peak at high binding energy becomes dominating and the peak at low binding energy almost disappears. This suggests that lattice oxygen is almost fully covered up by the adsorbed species or active oxygen species on the surface of the stored sample. According to previous reports, H_2O adsorption on NiO only happens when non-lattice oxygen is present [22] and CO_2 adsorption on metal oxides usually occurs in the site of active oxygen anions [23]. Obviously, the presence of active oxygen species takes a key role in the formation of adsorbed hydroxyl and carbonate species on the stored $LiNi_{0.8}Co_{0.2}O_2$.

In the Ni 2p spectra in Fig. 5, the dominating Ni $2p_{3/2}$ peak of fresh sample is at 856.0 eV, which corresponds to a Ni^{3+} as expected for $LiNi_{0.8}Co_{0.2}O_2$. For the stored sample, the Ni $2p_{3/2}$ peak becomes broader and is shifted to a lower position at 854.5 eV with a split into two peaks at 854.0 and 855.5 eV, respectively. This phenomenon is similar to that of NiO [24], suggesting that divalent nickel ion is the dominating format on the stored $LiNi_{0.8}Co_{0.2}O_2$. In other words, there is a reduction process of Ni^{3+} to Ni^{2+} on the $LiNi_{0.8}Co_{0.2}O_2$ during storage. This process causes the formation of active oxygen species, and is the possible trigger for the chemical reactions to form Li_2CO_3/LiOH, as described in previous work on $LiNiO_2$ [12]. On the contrary, the Co 2p spectra have no obvious change, and cobalt ions are kept in trivalence before and after storage. This result shows that the poorer storage property of $LiNiO_2$-based materials than that of $LiCoO_2$ most likely originate from the lower chemical stability of Ni^{3+} than that of Co^{3+} in the layered metal oxide frame.

XRD results gave more evidence of the surface structure changes on $LiNi_{0.8}Co_{0.2}O_2$ during the storage. As shown in Fig. 6, an obvious difference is that crystalline Li_2CO_3 phase appears in the pattern of the stored sample. Meanwhile, there are some changes in the intensity of the diffraction peaks

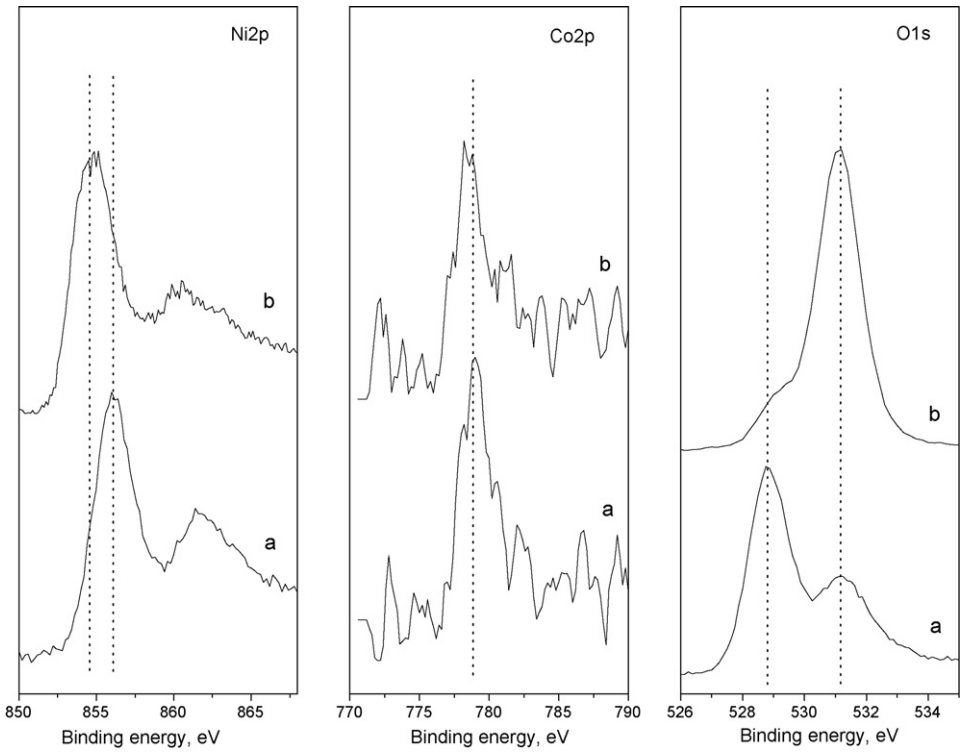

Fig. 5. Ni 2p and O 1s XPS spectra of $LiNi_{0.8}Co_{0.2}O_2$ materials: (a) fresh; (b) stored in air.

before and after storage. The intensity ratio of $I(0\,0\,3)/I(1\,0\,4)$ are 1.76 and 1.45, respectively, for the fresh and stored sample. The split degree of peak couples, i.e., (0 0 6)/(1 0 2) and (1 0 8)/(1 1 0), decreases considerably for the stored sample. Since these characteristic diffraction peaks were considered as the evidence of the degree of cationic disorder and lithium deficiency in $LiNiO_2$-based materials [25], some structure/composition changes should occur on $LiNi_{0.8}Co_{0.2}O_2$ during exposure to air. By Rietveld refinement with the model of $[Li_{1-x}Ni_x]_{3a}[Ni]_{3b}[O_2]_{6c}$, the amount of Ni_{3a} was found to increase from 0.053 for the fresh sample to 0.106 for the stored sample. This means that the degree of cationic disorder in the layered structure increases, and more nickel ions with inactive cubic rock salt phase appears in the stored sample. It is worthwhile to note that the Ni at Li 3a site should be divalent due to the difference of ionic radius ($r_{Ni^{3+}} = 0.56$ Å , $r_{Ni^{2+}} = 0.70$ Å , and $r_{Li^+} = 0.74$ Å). Thus, XRD results demonstrate that besides the formation of Li_2CO_3, the change of ionic distribution and the Ni^{3+}/Ni^{2+} transformation on $LiNi_{0.8}Co_{0.2}O_2$ during exposure to air also happened.

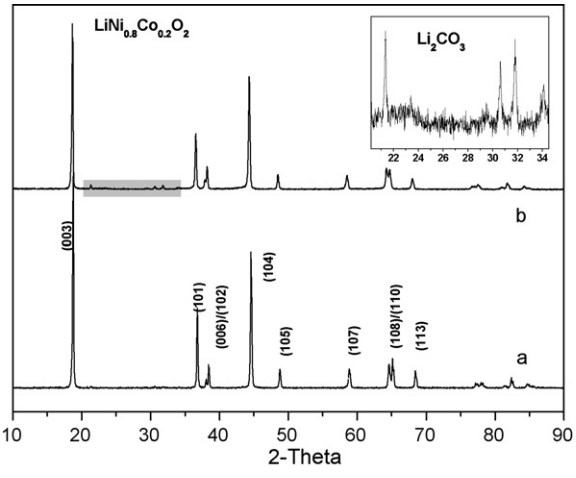

Fig. 6. XRD patterns of $LiNi_{0.8}Co_{0.2}O_2$ material: (a) fresh; (b) stored in air.

Abraham and coworkers [8] also observed the surface structure change on the stale $LiNi_{0.8}Co_{0.2}O_2$ by high resolution electron microscopy (HREM). In their experiments, a NiO-like thin layer (~4 nm) near surface region between the layer of adsorbed species and the bulk phase was found. Therefore, the surface changes on $LiNi_{0.8}Co_{0.2}O_2$ during storage in the air can be proposed briefly as follows. During storage, a reduction of Ni^{3+} to Ni^{2+} happens on the $LiNi_{0.8}Co_{0.2}O_2$ surface, accompanied with the formation of active oxygen species. The active oxygen species easily combine with H_2O and CO_2 in air to form adsorbed hydroxyl, carbonate and bicarbonate species. These adsorbed species further combine with surface Li^+ to form LiOH, $LiHCO_3$ and Li_2CO_3. Because of the consumption of oxygen atoms and Li^+ near the particle surface by the formation of carbonate species and Li_2CO_3 salt, a layer of the bulk hexagonal structure phase can be gradually turned into a NiO-like cubic phase. After a long period of exposure to air, beside the formation of a layer of adsorbed species (hydroxyl, carbonate and bicarbonate) and crystalline Li_2CO_3 on the surface, a NiO-like thin layer between the layer of adsorbed species and

bulk $LiNi_{0.8}Co_{0.2}O_2$ can also be formed. The overall possible surface reactions in the presences of trace H_2O and CO_2 can be proposed as follows:

$$LiNi_{0.8}Co_{0.2}O_2 + 0.4H_2O \rightarrow 0.8LiOH + 0.8NiO + 0.2LiCoO_2 + 0.2O_2\uparrow \quad (1)$$

$$LiOH + CO_2 \rightarrow LiHCO_3 \quad (2)$$

$$LiOH + LiHCO_3 \rightarrow Li_2CO_3 + H_2O \quad (3)$$

$$LiNi_{0.8}Co_{0.2}O_2 + 0.4CO_2 \rightarrow 0.4Li_2CO_3 + 0.8NiO + 0.2LiCoO_2 + 0.2O_2\uparrow \quad (4)$$

Apparently, both the layers are electrochemically inactive to lithium intercalation/deintercalation, which are believed to be responsible for the performance loss of the stored $LiNi_{0.8}Co_{0.2}O_2$.

3.4. Approaches to reduce the storage loss

Based on the reaction mechanism mentioned above, two approaches were proposed to improve the storage property of $LiNi_{0.8}Co_{0.2}O_2$ cathode material. The first one was to reduce or eliminate the reduction of Ni^{3+} to Ni^{2+}, which is the trigger for the whole surface reaction mechanism to form undesirable inactive layers on $LiNiO_2$-based materials. Reducing nickel content in the compound is an effective way to achieve that. For example, the storage loss of $LiNi_{0.8}Co_{0.2}O_2$ is much less than that of $LiNiO_2$ (Table 1), which is mainly due to the 20% (atomic weight) of Nickel content being replaced by cobalt. After 20% of nickel content reduction, the amounts of surface adsorbed species and Li_2CO_3 on the stored $LiNi_{0.8}Co_{0.2}O_2$ were much less than those on the stored $LiNiO_2$ (Fig. 3).

A further reduction of nickel content was achieved through synthesizing a new cathode material of $LiNi_{0.75}Ti_{0.05}Co_{0.2}O_2$ by adding 5% of titanium in the compound. Fig. 7 and also Table 1 show the storage property of $LiNi_{0.75}Ti_{0.05}Co_{0.2}O_2$ cathode material. As shown, the discharge specific capacity of this quaternary cathode material only lost 11% after storage in air for 6 months, while $LiNi_{0.8}Co_{0.2}O_2$ has a performance loss of 21% for the same conditions. These results indicate that doping other metal elements to replace nickel can suppress the reduction of Ni^{3+} to Ni^{2+} and thus effectively reduce the storage loss of $LiNiO_2$-based cathode materials.

Table 1
Data of charge and discharge specific capacity for various cathode materials

Samples	Specific capacity (mAh g^{-1})	
	Charge	Discharge
$LiNiO_2$[a]		
Fresh	215	160
Stored in air	113	70
$LiNi_{0.8}Co_{0.2}O_2$		
Fresh	202	180
Stored in Ar	190	168
Stored in air	167	142
$LiNi_{0.75}Ti_{0.05}Co_{0.2}O_2$		
Fresh	188	171
Stored in Ar	172	160
Stored in air	164	153
Stale $LiNi_{0.8}Co_{0.2}O_2$		
Heat-treated at 500 °C	185	164
Heat-treated at 725 °C	201	178

[a] The data were cited from Ref. [12] and tested in the range of 2.7–4.3 V.

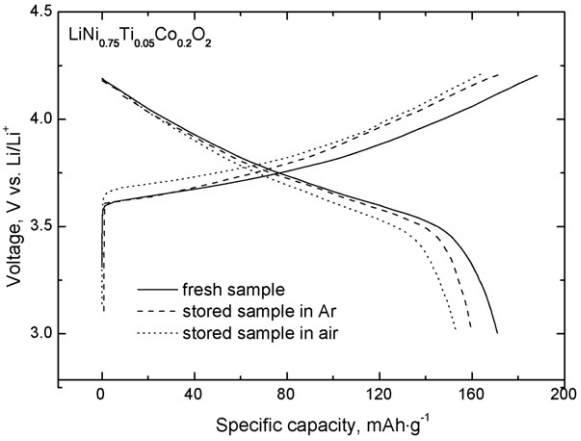

Fig. 7. Charge–discharge curves of $LiNi_{0.75}Ti_{0.05}Co_{0.2}O_2$ cathode material: (solid line) fresh; (dash line) stored in Ar; (dot line) stored in air.

The second approach is to isolate the cathode material from air. By isolating the material from H_2O and CO_2, the surface chemical reactions cannot happen even if a reduction trend of Ni^{3+}/Ni^{2+} exists on the $LiNi_{0.8}Co_{0.2}O_2$ particle surface. Figs. 1 and 7 and Table 1 have demonstrated that clearly by comparing the sample stored in air to that stored in Ar. Only 7% ($LiNi_{0.8}Co_{0.2}O_2$) and 3% ($LiNi_{0.75}Ti_{0.05}Co_{0.2}O_2$) storage losses can be observed, respectively, compared to those of the fresh samples. Therefore, storing cathode materials in an atmosphere without CO_2 and H_2O looks like an effective approach to improve the storage property of $LiNiO_2$-based materials.

3.5. Approaches to recover the storage loss

Storage loss recovery is another aspect that is practically important. According to the analysis above, the degraded performance of the stored materials is not only caused by the formation of surface adsorbed species and crystalline Li_2CO_3, but also contributed to the formation of a surface NiO-like thin layer. An effective approach to recover the storage loss should be the removal of both inactive layers on the particle surface. Water washing has been tried [7], and the removals of adsorbed carbonates and Li_2CO_3 seemed very effective. However, the washing process could create more NiO-like cubic phase due to the reaction of $LiNiO_2$ with H_2O.

Heat-treatment is another approach to decompose the adsorbed carbonate layer and re-oxide the NiO layer. Fig. 8 and also Table 1 show the charge–discharge data of the stored-in-air $LiNi_{0.8}Co_{0.2}O_2$ materials heat-treated at 500 and 725 °C in O_2 flow, respectively. As shown, after heat re-treatment at

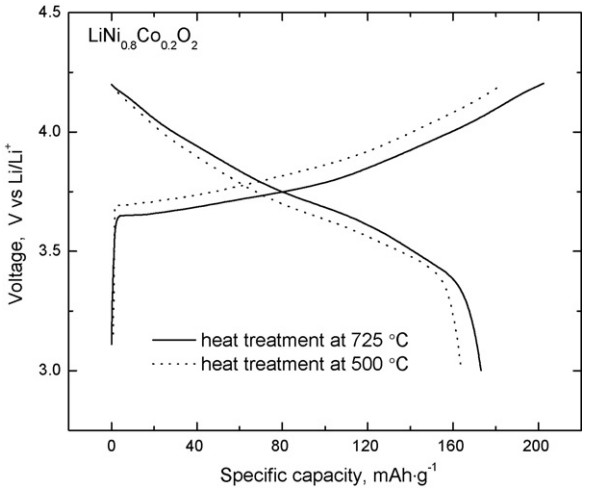

Fig. 8. Charge–discharge curves of the stored $LiNi_{0.8}Co_{0.2}O_2$ cathode material after heat treatment at 500 and 725 °C, respectively.

500 °C, the charge/discharge specific capacity of the stored sample is increased from 167/142 to 185/164 mAh g^{-1}. After heat-treatment at 725 °C, the charge/discharge specific capacity is further increased to 201/178 mAh g^{-1}, which almost reaches the level of the fresh sample (202/180 mAh g^{-1}). At 500 °C, only the adsorbed layer could be removed, and at 725 °C Li_2CO_3 and NiO were decomposed and re-oxidized, therefore, a full recovery can be achieved. This full recovery of storage loss clearly demonstrates the feasibility of a heat-treatment process.

4. Conclusions

$LiNi_{0.8}Co_{0.2}O_2$ cathode material showed a performance loss after exposure to air. Adsorbed hydroxyl, bicarbonate, carbonate, crystalline Li_2CO_3, and NiO-like species were identified to be the major species formed on the stored materials. The material particles covered by these species have poor conductivity towards Li^+ transfer and are electrochemically inactive, which are believed to be responsible for the storage loss.

It is proposed that during storage in air, a reduction of Ni^{3+} to Ni^{2+} on the particle surface could produce active oxygen species, which then react with trace H_2O and CO_2 in the air, and further combine with Li^+ to form LiOH, $LiHCO_3$ and Li_2CO_3. Meanwhile, a NiO-like thin layer was also formed between the adsorbed layer and bulk material due to the depletion of lithium and oxygen.

The storage loss of $LiNi_{0.8}Co_{0.2}O_2$ can be reduced by two approaches, i.e.: (1) decreasing the nickel content inside the compound through a doping approach and (2) storing the material in an inert atmosphere without H_2O and CO_2. For storage loss recovery, a heat-treatment process has been approved to be effective at 725 °C, at which a full recovery can be achieved.

Acknowledgements

This work was financially supported by the NSFC (National Natural Science Foundation of China) project (No. 29925310), NSERC (Natural Sciences and Engineering Research Council of Canada) postdoctoral fellowship, and NRC Institute for Fuel Cell Innovation. We also thank Ms. Marianne Rodgers for English proofreading.

References

[1] J.M. Tarascon, M. Armand, Nature 414 (2001) 361.
[2] C. Delmas, M. Menetrier, L. Croguennec, I. Saadoune, A. Rougier, C. Pouillerie, G. Prado, M. Grune, L. Fournes, Electrochim. Acta 45 (1999) 243.
[3] A. Ueda, T. Ohzuku, J. Electrochem. Soc. 141 (1994) 2010.
[4] Y. Gao, M.V. Yakovleva, W.B. Ebner, Electrochem. Solid-State Lett. 1 (1998) 117.
[5] A. D'Epifanio, G. Croce, F. Ronci, V.R. Albertini, E. Traversa, B. Scrosati, Phys. Chem. Chem. Phys. 3 (2001) 4399.
[6] K. Matsumoto, R. Kuzuo, K. Takeya, A. Yamanaka, J. Power Sources 81/82 (1999) 558.
[7] R. Moshtev, P. Zlatilova, S. Vasilev, I. Bakalova, A. Kozawa, J. Power Sources 81/82 (1999) 434.
[8] A.M. Andersson, D.P. Abraham, R. Haasch, S. MacLaren, J. Liu, K. Amine, J. Electrochem. Soc. 149 (2002) A1358.
[9] G.V. Zhuang, G. Chen, J. Shim, X. Song, P.N. Ross, T.J. Richardson, J. Power Sources 134 (2004) 293.
[10] J. Kim, Y. Hong, K.S. Ryu, M.G. Kim, J. Cho, Electrochem. Solid-State Lett. 9 (2006) A19.
[11] X.J. Zhu, H.H. Chen, H. Zhan, D.L. Yang, Y.H. Zhou, J. Mater. Sci. 40 (2005) 2995.
[12] H.S. Liu, Z.R. Zhang, Z.L. Gong, Y. Yang, Electrochem. Solid-State Lett. 7 (2004) A190.
[13] H.S. Liu, J. Li, Z.R. Zhang, Z.L. Gong, Y. Yang, J. Solid State Electrochem. 7 (2003) 456.
[14] H.S. Liu, J. Li, Z.R. Zhang, Z.L. Gong, Y. Yang, Electrochim. Acta 49 (2004) 1151.
[15] A.C. Larson, R.B. Von Dreele, General Structure Analysis System (GSAS), Los Alamos National Laboratory Report LAUR 86-748 (2004).
[16] G.X. Wang, J. Horvat, D.H. Bradhurst, H.K. Liu, S.X. Dou, J. Power Sources 85 (2000) 279.
[17] G. Busca, V. Lorenzelli, Mater. Chem. 7 (1982) 89.
[18] M.C. Manchado, J.M. Guil, A.P. Masi, A.R. Paniego, J.M. Menayo, Langmuir 10 (1994) 685.
[19] R. Philippt, K. Fujimoto, J. Phys. Chem. 96 (1992) 9035.
[20] M. Iwamoto, Y. Yoda, M. Egashira, T. Seiyam, J. Phys. Chem. 80 (1976) 1989.
[21] R. Gottschall, R. Schollhorn, Inorg. Chem. 37 (1998) 1513.
[22] J.M. Mckay, V.E. Henrich, Phys. Rev. B 32 (1985) 6764.
[23] D.E.A. Gordon, R.M. Lambert, Surf. Sci. 287/288 (1993) 114.
[24] A. Galtayries, J. Grimblot, J. Electron Spectrosc. Relat. Phenom. 98/99 (1999) 267.
[25] J. Morales, C.P. Vicente, J. Tirado, Mater. Res. Bull. 61 (1990) 623.